

ORIGINAL PAPER

Infectious Diseases

Comparison of pirfenidone and corticosteroid treatments at the COVID-19 pneumonia with the guide of artificial intelligence supported thoracic computed tomography

Murat Acat¹  | Pinar Yildiz Gulhan²  | Serkan Oner³  | Muhammed Kamil Turan⁴ 

¹Department of Pulmonary Diseases, Karabuk University, Karabuk Training and Research Hospital, Karabuk, Turkey

²Department of Chest Diseases, Duzce University Faculty of Medicine, Duzce, Turkey

³Department of Radiology, Bakircay University, Cigli Regional Training and Research Hospital, Izmir, Turkey

⁴Department of Medical Biology and Genetics, Karabuk University, Faculty of Medicine, Karabuk, Turkey

Correspondence

Pinar Yildiz Gulhan, Department of Chest Diseases, Duzce University Faculty of Medicine, Konuralp Campus, 81010 Duzce, Turkey.
Email: pinaryildiz691@hotmail.com

Funding information

None.

Abstract

Aim: We aimed to investigate the effect of short-term pirfenidone treatment on prolonged COVID-19 pneumonia.

Method: Hospital files of patients hospitalised with a diagnosis of critical COVID-19 pneumonia from November 2020 to March 2021 were retrospectively reviewed. Chest computed tomography images taken both before treatment and 2 months after treatment, demographic characteristics and laboratory parameters of patients receiving pirfenidone + methylprednisolone ($n = 13$) and only methylprednisolones ($n = 9$) were recorded. Pulmonary function tests were performed after the second month of the treatment. CT involvement rates were determined by machine learning.

Results: A total of 22 patients, 13 of whom (59.1%) were using methylprednisolone + pirfenidone and 9 of whom (40.9%) were using only methylprednisolone were included. When the blood gas parameters and pulmonary function tests of the patients were compared at the end of the second month, it was found that the FEV₁, FEV₁%, FVC and FVC% values were statistically significantly higher in the methylprednisolone + pirfenidone group compared with the methylprednisolone group ($P = .025$, $P = .012$, $P = .026$ and $P = .017$, respectively). When the rates of change in CT scans at diagnosis and second month of treatment were examined, it was found that the involvement rates in the methylprednisolone + pirfenidone group were statistically significantly decreased ($P < .001$).

Conclusion: Antifibrotic agents can reduce fibrosis that may develop in the future. These can also help dose reduction and/or non-use strategy for methylprednisolone therapy, which has many side effects. Further large series and randomised controlled studies are needed on this subject.

1 | INTRODUCTION

Following the reporting of new coronavirus (severe acute respiratory syndrome-coronavirus-2 (SARS-CoV-2)) pneumonia cases in Wuhan, Hubei, China in December 2019, the World Health

Organization (WHO) announced it as “a global epidemic” on 11 March 2020.¹

At the beginning of the pandemic, it was thought that possible mechanisms of complications might have been associated with the effects of SARS-CoV and MERS-CoV since SARS-CoV-2, the virus responsible for COVID-19, is from the same coronavirus family with SARS and Middle East Respiratory Syndrome (MERS) and that experience from these pulmonary

The manuscript has been read and approved by all the authors, that the requirements for authorship as stated earlier in this document have been met, and that each author believes that the manuscript represents honest work.

syndromes could be helpful in the treatment of the emerging COVID-19 outbreak.^{2,3}

The SARS-CoV-2 infection has infected more than 50 million people around the world. SARS-CoV-2 infection, in the most severe cases, can cause tissue hyperinflammation, fibrosis and scarring, lung collapse, multi-organ dysfunction and death. Severely affected survivors have a trail of devastating pulmonary fibrosis, which physicians will need to urgently address and manage. While fibrosis is a physiologic response to any pulmonary infection, chest physicians across the globe are encountering vast numbers of patients who have recovered from their acute COVID-19 pneumonia only to be left with severe residual lung fibrosis and oxygen dependence.^{4,5}

The presence of pulmonary fibrosis is probably a consequence of the cytokine storm. Some of these biological and pathological characteristics are shared with idiopathic pulmonary fibrosis (IPF) such as chronic inflammatory fibrotic lung disease caused by the synthesis and release of pro-inflammatory cytokines, including tumour necrosis factor alpha (TNF- α) and interleukin-1-beta (IL-1 β). Antifibrotic therapy with pirfenidone, a drug indicated for the treatment of IPF, could therefore play a key role in preventing serious or fatal lung complications. However, antifibrotic therapy could play an even more important role in combined regimens, once identified, with effective anti-inflammatory treatments. Combination therapy could act on the main anti-inflammatory and antifibrotic pathways in a synergistic way, mitigating the consequences of pulmonary fibrosis.⁶ Pirfenidone was approved as an anti-fibrotic in China in December 2013 for the treatment of IPF. The reduction in the overexpression of transforming growth factor β (TGF- β), connective tissue growth factor (CTGF), platelet-derived growth factors (PDGF) and TNF- α in inflammatory diseases plays a key role in the anti-fibrotic activity of pirfenidone.⁷

Currently, there is no clear evidence as to which treatment is effective for improving prognosis in patients infected with SARS-CoV-2. To date, a large number of clinical trials have been conducted for drugs showing *in vitro* efficacy. In this study, we aimed to demonstrate the results of short-term (2 months) pirfenidone treatment in prolonged COVID-19 pneumonia, which has no effective treatment yet.

2 | MATERIALS AND METHODS

2.1 | Study population

In this study, the information of patients hospitalised with a diagnosis of critical COVID-19 pneumonia from November 2020 to March 2021 were retrospectively obtained from the hospital system. Chest CT images were taken both before treatment and 2 months after treatment, demographic characteristics and laboratory parameters of patients receiving pirfenidone + methylprednisolone ($n = 13$) and only methylprednisolones ($n = 9$) were recorded. Mild, moderate, and severe cases were not included. Additionally, we excluded the patients under 18 years of age and pregnant women. Patients were

What's known

- The SARS-CoV-2 infection has infected more than 50 million people around the world.
- Severely affected survivors have a trail of devastating pulmonary fibrosis, which physicians will need to urgently address and manage.

What's new

- Post-COVID fibrosis, may continue to be a challenge for physicians even after the pandemic.
- Antifibrotic agents can reduce fibrosis that may develop in the future.
- Also, these can help dose reduction and/or non-use strategy for methylprednisolone therapy, which has many side effects.

classified according to the WHO classification system (WHO/2019-nCoV/clinical/2021.1). Patients who received pirfenidone treatment 2 weeks after the diagnosis of COVID-19 were included.

2.2 | Treatments

Favipiravir, 3 days of high dose methylprednisolone (250 mg) followed by 0.5 mg/kg/d, and anticoagulant treatment were administered to all patients. The pirfenidone treatment was increased to a maximum of 2400 mg with weekly dose increments.

2.3 | Pulmonary function test

Pulmonary function tests were performed in the second month of the treatment. The tests were performed using a standard spirometer (Spirolab[®]-2) according to American Thoracic Society criteria while the patients were at rest and seated in the upright position. Forced vital capacity (FVC), forced expiratory volume in 1 second (FEV1) and FEV1/FVC (%) were measured. Results were expressed as absolute values and percentages of predictive values.

2.4 | Chest computed tomography protocols

Chest CT scans were conducted with a 16-detector spiral CT scanner (Toshiba Alexion, Otawara, Japan) in the full inspiration phase in the supine position. Patients were instructed to hold their breath to minimise motion artefacts. CT images were created by taking axial sections with 256 \times 256 matrix size and 3 mm reconstructed 5 mm section thickness. Tube voltage was 120 kVp, rotation time was 0.75 seconds, and pitch was 1 mm. The low-dose CT protocol available in the scanner was used in the standard setting for the

scans (AIDR3D, Canon Medical Systems, Ōtawara, Japan). Average CTDIvol was 3.3 mGy (range: 2.2–4.9 mGy). Implementation of appropriate infection prevention and control measures were arranged in all suspected CT cases, consisting of prompt sanitation of CT facility and patient's isolation.

2.5 | Image analysis

Each patient had varying degrees of CT findings for COVID-19 pneumonia identified in previous studies^{8,9} such as ground-glass opacities, consolidation, crazy-paving pattern, reticular pattern, air bronchogram, vascular enlargement in the lesion, centrilobular nodules, airway changes (bronchiectasis and bronchial wall thickening), pleural changes (pleural effusion and pleural thickening), subpleural curvilinear line, air bubble sign, intrathoracic lymph node enlargement, nodules, halo sign, reversed halo sign and pericardial effusion. These findings were double-blindly confirmed by a radiologist (SO) with at least 10 years of experience in the field. Images in parenchyma dose were taken from the hospital archive in DICOM format and transferred to the workstation for volumetric analysis.

Segmentation is divided into two parts as preprocessing and processing. Reading DICOM images, obtaining patient and image characteristics, creating Hounsfield Matrix from 16-bit DICOM images, and transforming matrices to the best image windows are performed during preprocessing. Detection of ROI for chest wall, lung segmentation, calculation of all threshold values with randomised cascade mean filter method, image enhancement and obtaining ROI on enhanced images are performed during processing.

Images are transformed into soft tissue window to obtain the ROI of lungs. Therefore, pixel values of lungs are normalised to window minimum. Minimum filter is applied on soft tissue window and lungs are obtained on binary images. Hilar area, bronchi, broncholar, and pulmonary vessels are classified as lungs by filling blanks on

binary images. Median filter is applied to remove small noises and artefacts. As a result, a mask is obtained for lungs. After, a sectional image view is taken into lung window and multiplied with mask values. As a result, the obtained image is a lung image that has suitable conditions to process. Sample images obtained after these processes are shown in Figure 1.

All possible threshold values were calculated with randomised cascade mean filter to enhance lung images that have suitable conditions to process in terms of contrast. In this study, length parameter was specified as 20 and repetition number parameter was specified as 10% of mask area. Randomised selected lines on images were generated using these parameters. These lines have pixel values on images. The mean of sequential two-pixel values on the lines were taken until only one value was obtained. The obtained value was assigned as the threshold value.^{10,11} Lung images were converted to binary images using all possible threshold values. Then, all binary images were added on themselves. As a result, lung images with suitable conditions to process were enhanced in terms of contrast. A sample is shown in Figure 2.

Randomised cascade mean filter was applied again on the enhanced lung images to obtain binary images and ROIs. The threshold value was obtained by taking the arithmetic mean of all possible threshold values calculated in the previous process. Areas with a pixel value of 1 were calculated. Areas with values are greater than 50 were labelled as ROIs. The labelled ROIs are shown in Figure 3.

Images whose ROIs were segmented were classified by radiologists and chest disease specialists using a developed graphical user interface. Three classes were used in this study. The first class includes ground-glass opacities. The second class includes COVID lesions seen such as consolidation, air bronchogram, vascular enlargement in the lesion, centrilobular nodules, subpleural curvilinear line or reticular pattern. The third class includes vessels and bronchi. Sample images belonging to these classes are shown in Figure 4.

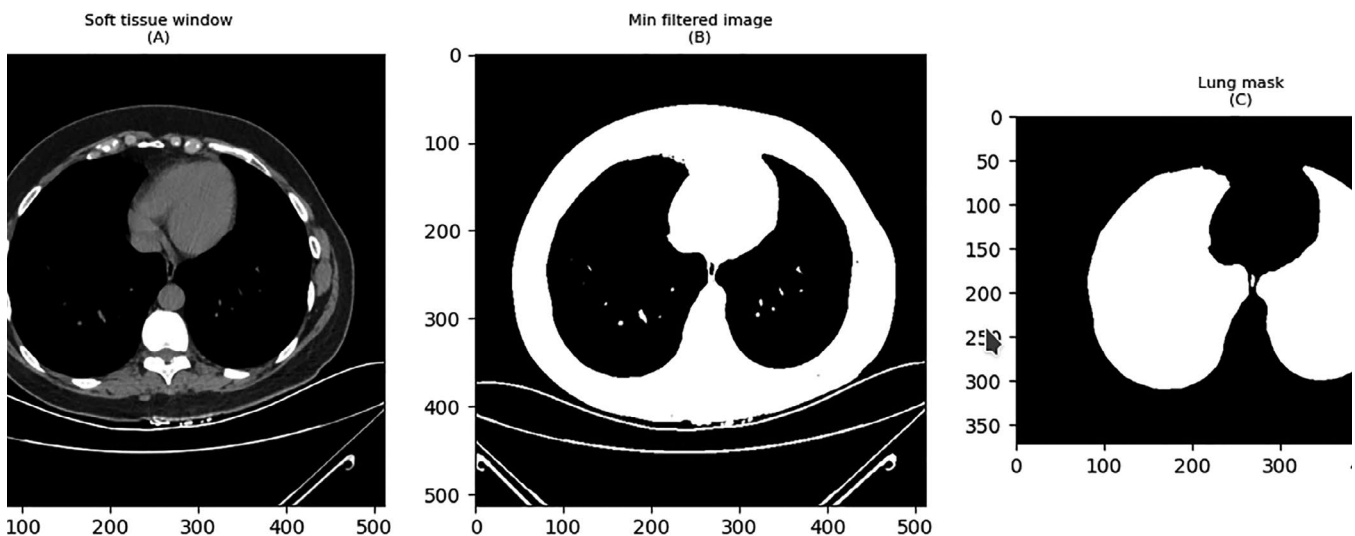


FIGURE 1 Images obtained after the processes. A, Soft tissue window image; B, Binary image obtained after minimum filter; C, Image obtained after the developed filters

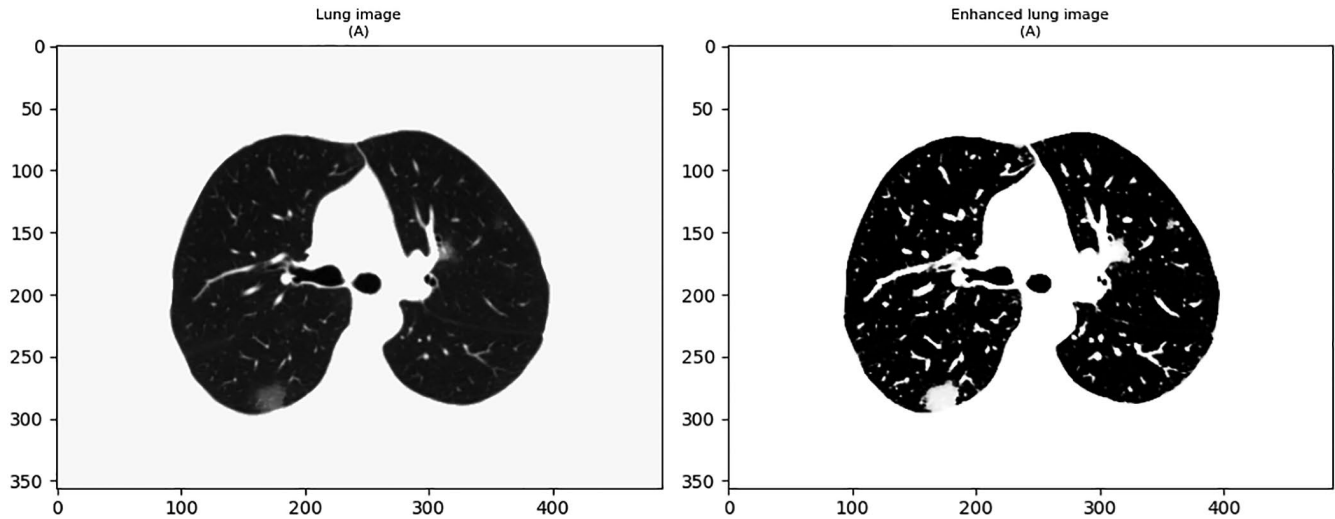


FIGURE 2 A sample image, (A) Lung images that have suitable conditions to process, (B) Enhanced lung image

Finally, the volumes of all classes were summed and the ratio to the total lung volume was calculated. Thus, estimated lung involvement rates were obtained on CT images before and after treatment.

2.6 | Decision system

1890 ROIs were obtained using all CT images in this study. Specialists classified the obtained ROIs on CT images. Feature extraction was done based on parameters from Gray Level Cooccurrence Matrix (GLCM). Therefore, input vector was obtained for machine learning algorithms. Four difference angles of 0 , $\pi/2$, π and $3\pi/4$ were used while calculating the GLCM parameters of contrast, dissimilarity, homogeneity, angular second moment (ASM), energy and correlation. These parameters were calculated for each angle value^{12,13}. Besides, minimum, maximum, mean, standard deviation and area value of pixel intensity values belonging to ROIs were calculated and added into input vector as new features. Also, eccentricity, major axis length, minor axis length and orientation values were calculated and added into input vector as new features.

Input vector used in machine learning algorithms includes 33 parameters. k-Nearest Neighbors (KNN), decision tree (DT), random forest (RF), extra tree classifier (ETC), gaussian naive Bayes (GNB), Ada boost classifier (ADA), gradient process classifier (GPC), linear discriminant analysis classifier (LDA) and quadratic discriminant analysis classifier (QDA) algorithms are used as machine learning algorithms. Accuracy (Acc), sensitivity (Sen) and specificity (Spe) based on confusion matrix and Mathew's correlation coefficient (MCC) are used to calculate the performance features of machine learning algorithms and compare them. Algorithms whose MCC values are higher than others are assigned as successful algorithms.

The most successful one among the three algorithms with the highest MCC value is identified by a majority voting system. In the use of machine learning algorithms, 80% of input vectors are identified as training set and 20% of input vectors are identified as test set. k value for k-fold cross validation is selected as 500. As a result, different training sets and test sets are obtained and performances of machine learning algorithms are calculated more accurately. Equations (1)-(4) present the parameters based on the confusion matrix:

$$\text{Acc} = \frac{\text{TP}}{\text{TP} + \text{FN} + \text{FP} + \text{TN}} \quad (1)$$

$$\text{Sen} = \frac{\text{TP}}{\text{TP} + \text{FN}} \quad (2)$$

$$\text{Spe} = \frac{\text{TN}}{\text{TN} + \text{FP}} \quad (3)$$

$$\text{Mcc} = \frac{\text{TP} \cdot \text{TN} - \text{FP} \cdot \text{FN}}{\sqrt{(\text{TP} + \text{FP}) \cdot (\text{TP} + \text{FN}) \cdot (\text{TN} + \text{FP}) \cdot (\text{TN} + \text{FN})}} \quad (4)$$

Equations (1)-(4): TP = true positive; TN = true negative; FP = false positive; FN = false negative.

2.7 | Ethical approval

The study was approved by both the Ministry of Health and the Local Ethics Committee (Karabuk University Local Ethic Committee approval document dated March 3, 2021 and numbered 2021/477). The patients were given an informed consent form and their written consent was obtained.

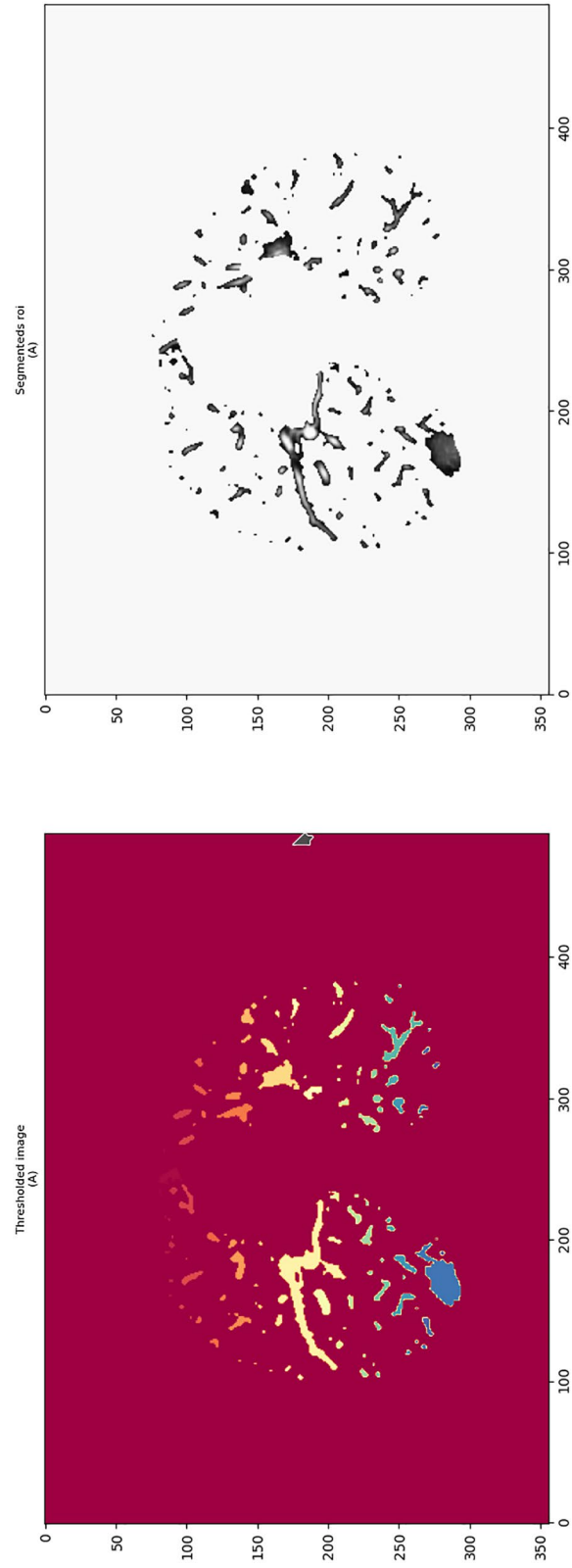


FIGURE 3 A sample image, (A) The thresholded image by randomized cascade mean filter, (B) The image whose ROIs are segmented

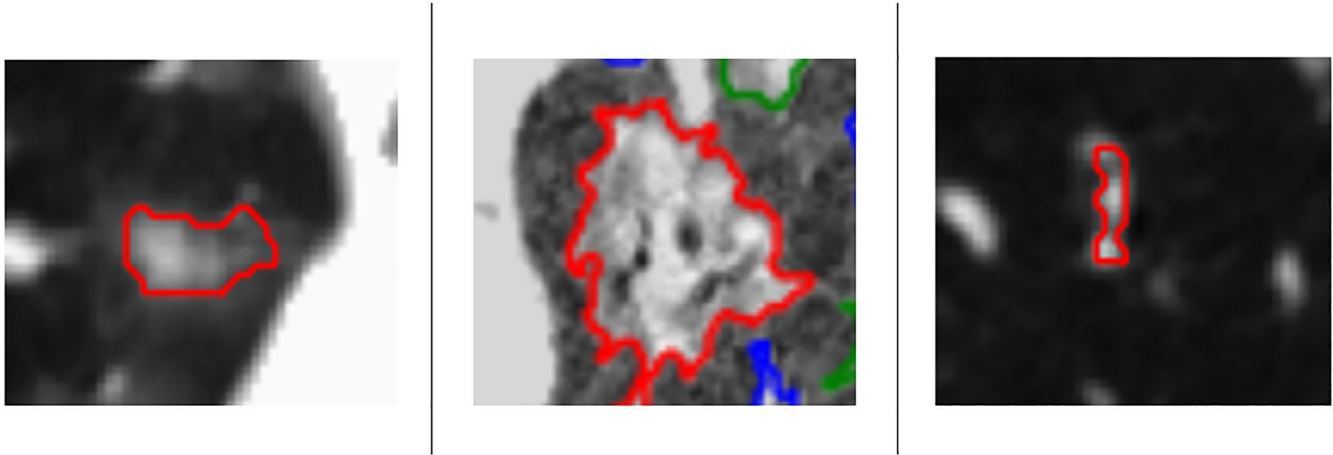


FIGURE 4 Automated lung segmentation. Respevcively, Covid lesion (ground-glass opasity), COVID lesion (consolidation), and vessels

2.8 | Statistical analysis

Categorical variables are presented as percentage and frequency. The chi-squared test and, where appropriate, Fisher's exact test were used to compare categorical variables between groups. The conformity of continuous variables to normal distribution was checked by visual histograms and the Shapiro-Wilk test. Normally distributed continuous variables are presented as mean \pm standard deviation, while non-normally distributed continuous variables are presented as median and IQR (interquartile range). Comparison of continuous variables between groups was performed using the independent samples t-test in normal distribution and the Mann-Whitney U test in non-normal distribution. The Repeated Measures test was used to compare the changes in the involvement rates of the groups at diagnosis and at the second month of treatment. All p values presented are two-sided and $P < .05$ was considered statistically significant. Statistical analyses were performed using the SPSS 26.0 (IBM Corp. 2019 IBM SPSS Statistics for Windows, version 26.0. Armonk, NY: IBM Corp) package software.

3 | RESULTS

A total of 22 patients, 13 of whom (59.1%) were using methylprednisolone + pirfenidone and 9 of whom (40.9%) were using only methylprednisolone were included. All patients in both groups received methylprednisolone, high-dose methylprednisolone and favipiravir treatment during their hospitalisation. None of our patients received tocilizumab treatment (Table 1). When patients' baseline laboratory parameters and hospitalisation periods were compared, it was found that the two groups were similar to each other ($P > .05$) (Table 2).

Comparing blood gas values at the time of discharge, the pH value of the group receiving methylprednisolone + pirfenidone was found to be statistically significantly lower ($P = .003$). Other blood gas parameters were found to be similar between the two groups ($P > .05$) (Table 3).

When the blood gas parameters and pulmonary function tests of the patients were compared at the end of the second month, it was found that the HCO₃, FEV₁, FEV₁%, FVC and FVC% values were statistically significantly higher in the group receiving methylprednisolone + pirfenidone compared with the group receiving only methylprednisolone ($P = .049$, $P = .025$, $P = .012$, $P = .026$ and $P = .017$, respectively). The second month pH, pO₂, pCO₂, saturation and MEF values were found to be similar between the groups ($P > .05$). Table 4 shows the comparison of the groups in terms of blood gas and pulmonary function tests in the second month after discharge.

The involvement rates in CT scans at diagnosis and second month of treatment were similar among the groups ($P = .073$ and $P = .477$, respectively). However, when the rates of change in CT scans at diagnosis and second month of treatment were examined, it was found that the involvement rates in the methylprednisolone + pirfenidone group were statistically significantly decreased ($P < .001$) (Figure 5). The comparison of the involvement rates between the groups at diagnosis and second month of treatment are presented in Table 5 and the sample patients are presented in Figures 6 and 7. The comparison of the change in the involvement rates of the groups is shown in Figure 1.

The performance of the decision system has been tested on the sections that were not shown to the system during training and reserved for testing, and the overall Acc value was calculated as 0.953. The performance metrics of the proposed method to make a final decision are shown in Table 6.

4 | DISCUSSION

We found a significant difference in the percentages of pulmonary parenchymal involvement between the patients hospitalised with the diagnosis of critical COVID-19 pneumonia using only methylprednisolone and using methylprednisolone and pirfenidone. There was no difference in pre-treatment pulmonary involvement between the groups. Parenchymal involvement after two months

TABLE 1 The general characteristics of the patients, the treatments and lung involvement rates

	Comorbidities										SpO ₂			Treatments				Lung Inv.R.	
	Sex	Age	DM	HT	CLD	CRD	M	CVD	in. SpO ₂	Con. SpO ₂	Hos.P	Fav	MP or P + MP	Ana	NIVM	Before	After		
1	F	58	Y	Y	N	N	N	N	67	88	49	Y	MP	Y	Y	0.25	0.24		
2	F	76	N	Y	N	Y	N	N	71	94	30	Y	P + MP	Y	Y	0.48	0.28		
3	M	78	N	N	N	N	N	N	81	93	22	Y	MP	Y	N	0.25	0.22		
4	M	52	N	N	N	N	N	N	85	97	15	Y	P + MP	Y	N	0.13	0.11		
5	F	78	N	N	N	N	N	N	75	94	15	Y	MP	N	N	0.29	0.26		
6	F	72	Y	Y	N	N	N	N	68	95	36	Y	MP	N	Y	0.13	0.26		
7	M	62	N	N	N	N	N	N	80	96	36	Y	MP	Y	Y	0.22	0.24		
8	M	56	Y	N	N	N	N	N	74	95	22	Y	MP	N	Y	0.36	0.25		
9	M	59	N	Y	N	N	N	Y	62	94	29	Y	P + MP	N	Y	0.36	0.23		
10	M	78	Y	Y	N	N	N	N	69	90	35	Y	P + MP	N	Y	0.35	0.26		
11	M	71	N	N	N	N	N	N	81	91	16	Y	P + MP	Y	N	0.29	0.23		
12	M	72	Y	Y	N	N	N	N	89	96	25	Y	MP	N	N	0.28	0.27		
13	M	64	Y	Y	N	N	Y	N	76	94	17	Y	P + MP	N	N	0.36	0.28		
14	F	38	N	N	N	N	N	N	65	97	24	Y	P + MP	N	Y	0.31	0.12		
15	M	69	Y	Y	N	N	N	Y	85	94	19	Y	P + MP	N	Y	0.38	0.28		
16	M	78	N	N	N	N	N	N	80	82	26	Y	P + MP	N	N	0.39	0.24		
17	M	70	N	Y	N	N	N	N	88	96	19	Y	P + MP	N	N	0.2	0.15		
18	M	67	N	N	N	N	N	N	86	96	28	Y	P + MP	N	N	0.27	0.24		
18	M	60	N	Y	N	N	N	N	87	95	7	Y	P + MP	N	N	0.16	0.15		
20	M	65	N	Y	N	N	N	N	68	95	21	Y	P + MP	Y	Y	0.28	0.15		
21	M	75	N	Y	N	N	Y	N	72	98	22	Y	MP	N	N	0.25	0.35		
22	M	62	N	N	N	N	N	N	75	96	23	Y	MP	N	N	0.18	0.26		

Abbreviations: Ana, anakinra; CLD, chronic lung disease; Con. SpO₂, control oxygen saturation level in the blood; CRD, chronic renal disease; CVD, cardiovascular disease; DM, diabetes mellitus; F/M, female/male; Fav, favipiravir; Hos.P, hospitalisation periods; HT, hypertension; in. SpO₂, initial oxygen saturation level in the blood; Lung Inv.R., lung involvement rates; M, malignancy; MP, methylprednisolone; N, No; P, pirfenidone; Y, yes.

Parameter	Methylprednisolone + Pirfenidone (n = 13)	Methylprednisolone (n = 9)	P
Leukocyte (K/mm ³)	9831 ± 4487	12 094 ± 3980	.238*
HB (g/dL)	12.8-1.65	14.2-2.35	.151**
PLT(K/mm ³)	292-136	260-157	.301**
Lymphocyte (mcL)	423.1 ± 135.8	447.6 ± 133.6	.679*
CRP (mg/dL)	167.09 ± 47.6	171.1 ± 55.8	.858*
Ferritin (ng/mL)	812.9-1027	679-769	.764**
LDH (U/L)	540-143	707-328	.151**
d-dimer (mcg/mL)	3.31-6.86	5.9-13.1	.526**
Hospitalisation periods (d)	21-12	23-14	.228**

Abbreviations: CRP, C-reactive protein; HB, hemoglobin; LDH, lactate dehydrogenase; PLT, platelet; SpO₂, oxygen saturation level in the blood.

*Independent samples t test.; **Mann-Whitney U test.

TABLE 2 Comparison of basal laboratory characteristics and hospitalisation periods of patient groups

Blood gas parameters	Methylprednisolone + pirfenidone (n = 13)	Methylprednisolone (n = 9)	P
pH	7.43 ± 0.03	7.48 ± 0.02	.003*
pO ₂ (mmHg)	51.86 ± 9.8	51.36 ± 11.8	.916*
pCO ₂ (mmHg)	40.3-7.6	36.2-3.05	.088**
HCO ₃ (mmol/L)	24.3-7.5	26.7-2.35	.442**
SpO ₂	81.91 ± 10.1	81.27 ± 8.4	.878*

Abbreviations: HCO₃, bicarbonate; PaCO₂, partial carbon dioxide pressure; PaO₂, partial oxygen pressure; SpO₂, oxygen saturation level in the blood.

*Independent samples t test.; **Mann-Whitney U test.

TABLE 3 Comparison of blood gas parameters of groups at the time of discharge

Parameters	Methylprednisolone + pirfenidone (n = 13)	Methylprednisolone (n = 9)	P
pH	7.41-0.05	7.42-0.04	.660**
pO ₂ (mmHg)	78.99 ± 12.9	78.41 ± 11.2	.914**
pCO ₂ (mmHg)	37.7-4.55	35.6-5.45	.077**
HCO ₃ (mmol/L)	24.1-3.65	22.9-3.2	.049**
SpO ₂	94.3-4	95.2-2.95	.639**
FEV1 (L)	2.33 ± 0.66	1.72 ± 0.44	.025**
FEV1 (% predicted)	83 ± 17.2	65.44 ± 9.3	.012**
FVC (L)	2.76 ± 0.8	2.01 ± 0.4	.026**
FVC (% predicted)	77.23 ± 17.9	60.22 ± 8.8	.017**

Abbreviations: FEV1, forced expiratory volume at 1 s; FVC, forced vital capacity; HCO₃, bicarbonate; PaCO₂, partial carbon dioxide pressure; PaO₂, partial oxygen pressure; SpO₂, oxygen saturation level in the blood.

*Mann-Whitney U test.; **independent samples t test.

TABLE 4 Comparison of the groups in terms of blood gas and pulmonary function tests at 2 mo after discharge

of treatment was statistically significantly less in the pirfenidone + methylprednisolone group compared with the methylprednisolone group. Also, comparing the pulmonary function tests of the patients in the second month, FEV1, FEV1%, FVC and FVC% values were found to be statistically significantly higher in the methylprednisolone + pirfenidone group than in the methylprednisolone group.

Unlike the SARS and MERS outbreaks having affected only a few thousand people, doctors are more likely to encounter many patients (potentially hundreds of thousands) who could develop post-COVID interstitial lung disease, as the current pandemic affects millions.⁴

The aetiology of pulmonary fibrosis is multifactorial and depends on age, smoking, viral infection, drug exposure and genetic

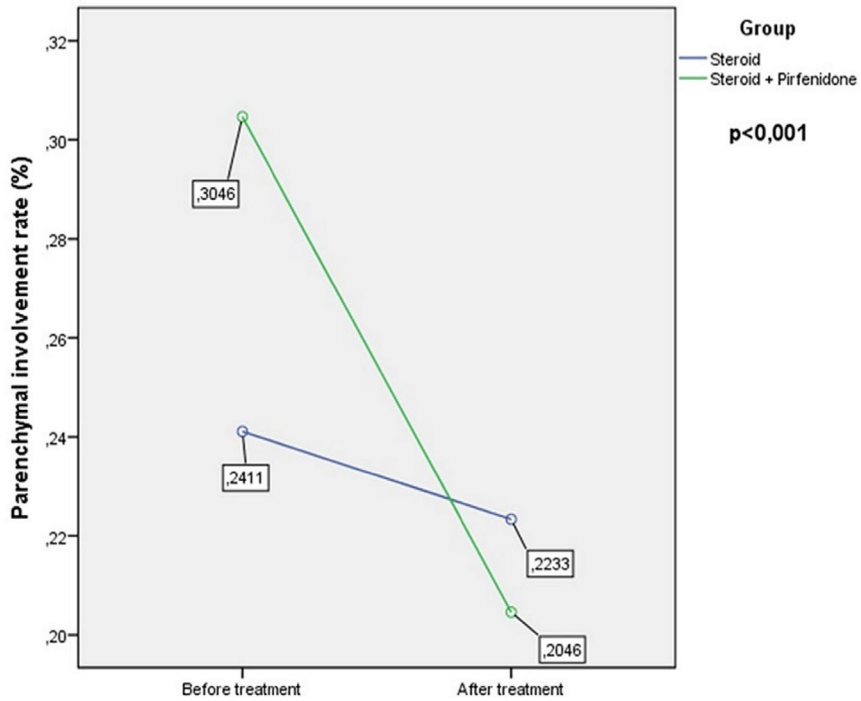


FIGURE 5 Comparison of the changes in the lung involvement rates of the groups

TABLE 5 Comparison of the before treatment and 2nd month involvement rates of the groups

Involvement rates (%)	Methylprednisolone + pirfenidone (n = 13)	Methylprednisolone (n = 9)	P
Before treatment	0.305 ± 0.08	0.241 ± 0.06	.073*
After treatment	0.205 ± 0.06	0.223 ± 0.05	.477*

*Independent samples t test.

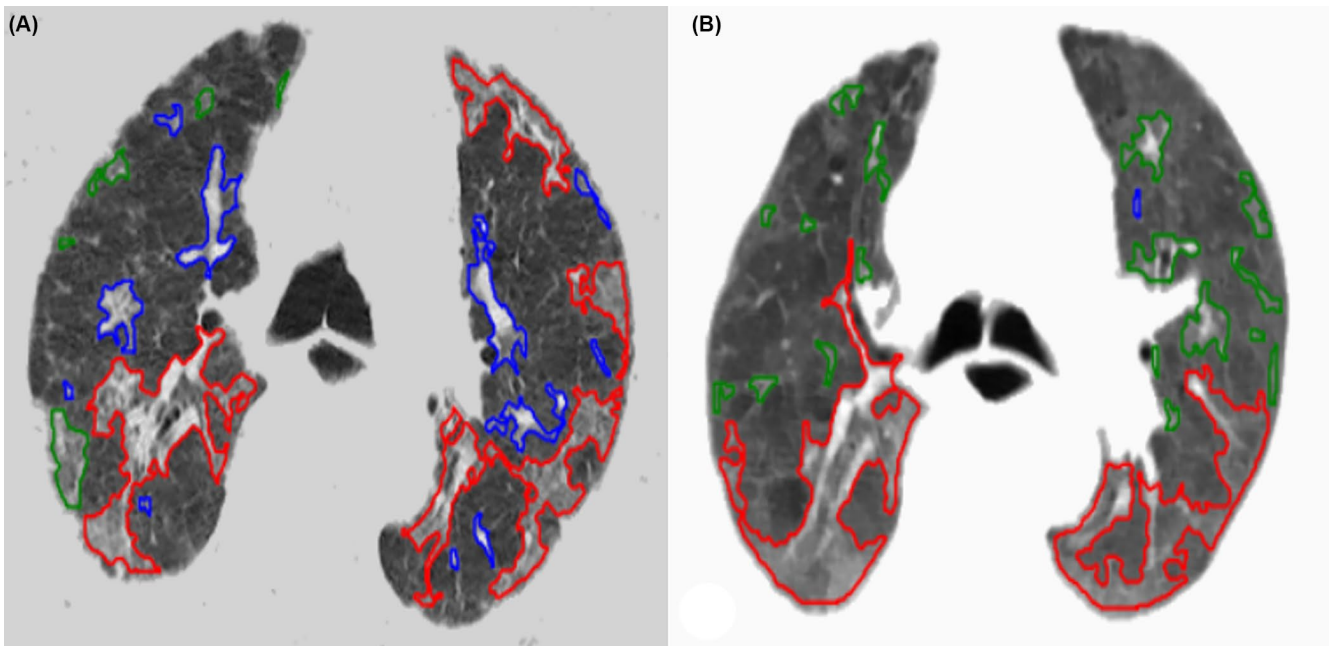


FIGURE 6 A male patient on methylprednisolone therapy; There is a slight decrease in the rates of lung involvement in CT images passing at the same level before (A) and after treatment (B)

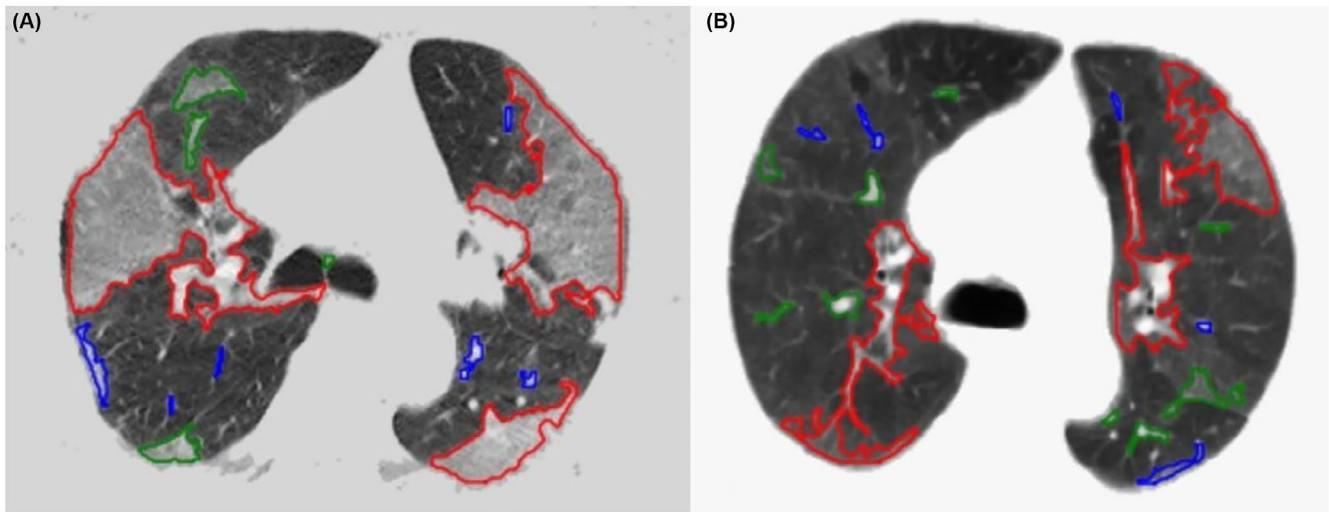


FIGURE 7 The male patient received methylprednisolone + pirfenidone treatment; Pre-treatment (A) and post-treatment (B) CT images that pass at the same level show a marked decrease in lung involvement rates

TABLE 6 The performance metrics of the proposed method

Algorithm	Class	Acc	Sen	Spe	Mcc
The proposed method	Ground-glass opacity	0.939	0.950	0.933	0.878
	Consolidation and other lesions	0.968	0.975	0.951	0.920
	Vessels and bronchi	0.944	0.961	0.885	0.953

Abbreviations: Acc, Accuracy; Mcc, Matthews correlation coefficient; Sen, Sensitivity; Spe, Specificity.

predisposition.^{14,15} No statistically significant difference was found between the ages of the patients included in this study.

In fibrosis in COVID-19 infection, inflammatory mediators such as transforming growth factor (TGF-beta), vascular endothelial growth factor (VEGF), interleukin 6 (IL-6) and tumour TNF- α are likely to occur because of the initiation of the fibrotic cascade. Moreover, vascular dysfunction causes the progression of fibrosis.^{16,17} Uncontrolled and excessive reaction of the immune system to the virus leads to the release of multiple inflammatory cytokines, increased production of superoxide, development of acute respiratory distress syndrome (ARDS) and subsequent matrix remodelling, and overproduction of collagens and other matrix components that can cause fibrosis in survivors.¹⁸

Studies have shown that the SARS-CoV-2 infection continues to cause further damage, possibly leading to fibrosis in the lung.^{19,20}

Tse et al histologically examined the pulmonary pathology of seven patients who died from SARS (hospitalisation periods: 4-20 days) and observed significant pulmonary oedema, hyaline membrane formation and widespread alveolar damage in all patients and mild to moderate fibrosis interstitial fibrosis in some regions.²¹

Zhang et al followed 71 SARS patients for 15 years. They demonstrated that interstitial abnormalities and functional decline resolved within the first 2 years after infection and then remained stable. At 15 years, 4%-6% of patients infected with SARS showed interstitial abnormality.²² Follow-up results with MERS

are less defined. In a study on 36 patients recovering from MERS, chest X-rays were taken an average of 43 days after discharge. One-third of patients showed abnormalities defined as lung fibrosis.²³ Longer follow-up of patients recovering from MERS has not been reported.²⁴ These studies have shown that persistent findings occur after SARS-CoV and MERS infections. It would not be wrong to predict that there may be long-term damage in patients after COVID-19 because of damage in diseases caused by previous coronaviruses.

Huang et al examined patients who survived a severe COVID-19 infection (at least 3 CT scans) and discovered findings consistent with fibrosis in 42 patients (extensive and persistent fibrotic changes, including parenchymal bands, irregular interfaces, reticular opacities and traction bronchiectasis with or without honey combing).²⁵

Fang et al examined the final follow-up of 12 patients hospitalised in the intensive care unit (mean ICU stay: 6.1 ± 7.7 days) and observed dominant reticulation and interlobular thickening in 8 patients on thoracic CT.²⁶

Mo et al evaluated pulmonary function tests after COVID-19 infection and noted anomalies in DLCO% predicted in 51 cases (47.2%), total lung capacity (TLC)% in 27 (25.0%), forced expiratory volume in 1 seconds (FEV1)% in 15 (13.6%), forced vital capacity (FVC)% in 10 (9.1%), FEV1/FVC in 5 (4.5%) and small airway function in 8 (7.3%).¹⁷

Güler²⁷ et al reported the long-term (4 months) results of COVID-19 infection and found DLCO reduction, radiological abnormalities and minor airway disease after severe acute SARS-CoV-2 infection. Since there was no diffusion test in our hospital, we evaluated it by FEV1, FVC% and FEV1 and found statistically significantly higher pulmonary function tests in the pirfenidone + methylprednisolone group compared with the methylprednisolone group.

Chaudhary et al stated that losing time, energy and resources for consent-weary patients was unnecessary. They stated that existing antifibrotics are for the management of chronic diseases, are not curative and do not reverse fibrosis. Since survivors have a lower prevalence of significant scarring and favourable course, they stated that there is no sufficient scientific rationale for antifibrotic drug use.²⁸ However, it was also considered that SARS-CoV-2 infection causes fibrosis in many ways, including the mechanism of ACE-2 receptors.²⁹

Diverse action mechanisms have been suggested for pirfenidone, among which are downregulating effects on a series of cytokines, including (TGF)- β 1, CTGF, PDGF and TNF- α .^{18,30,31} Besides, pirfenidone is a reactive oxygen species (ROS) scavenger, and last but not least, it downregulates the expression of ACE receptor, the major cellular receptor for COVID-19. Also, some other characteristics of pirfenidone make it an appropriate treatment for COVID-19, including its anti-apoptotic and anti-fibrotic effects.^{18,32-34} Pirfenidone can prevent lung injury during SARS-CoV-2 infection by blocking the maturation process of transforming growth TGF- β and enhancing the protective role of peroxisome proliferator-activated receptors (PPARs). Pirfenidone is a safe drug for patients with hypertension or diabetes and its side effects are well tolerated.³⁵

Momen⁷ et al reported that they used pirfenidone in five cases, not only during the PC-fibrosis period but also during COVID-19 pneumonia, as in our study. In a recent study, Umemura et al investigated the efficacy of nintedanib, an intracellular inhibitor of tyrosine kinases, in COVID-19 patients. They compared 30 patients who received nintedanib and 30 who did not. They did not find any significant difference in 28-day mortality but the lengths of MV were significantly shorter than the control group. CT scans were not different between two groups at baseline. However, the follow-up CT scan after leaving MV showed that percentages of high-attenuation areas were significantly lower in the nintedanib group. They stated that using an antifibrotic agent may be beneficial.³⁶ The involvement rates in CT scans at diagnosis and second month of treatment were similar. However, when the rates of change were examined, it was found that the involvement rates in the methylprednisolone + pirfenidone group were statistically significantly decreased ($P < .001$) (Figures 6 and 7).

Although there is only one case series¹² in the literature on pirfenidone, clinical studies are ongoing on the anti-inflammatory and antifibrotic effects of pirfenidone. At present, four clinical trials have been registered (<https://clinicaltrials.gov>) to assess the pirfenidone as a clinical treatment for patients affected by COVID-19 (<https://clinicaltrials.gov/ct2/results?cond=Covid-19+pirfenidone>). One of

these clinical trials included treatment with antifibrotic agents pirfenidone and nintedanib.

One limitation of our study was the small patient population. Patients who received methylprednisolone treatment were taken as the control group and we had no placebo group that did not receive any treatment. Regarding pulmonary function tests, the diffusing capacity of the lung for carbon monoxide (DLCO) could not be evaluated.

In conclusion, it is too early to reliably define long-term outcomes in patients recovering from a severe COVID-19 pneumonia. However, it is possible that the long-term complications of the COVID-19 pandemic, which affects millions, such as PC-fibrosis, may continue to be a challenge for physicians even after the pandemic. Antifibrotic agents can reduce fibrosis that may develop in the future. Also, these can help dose reduction and/or non-use strategy for methylprednisolone therapy, which has many side effects. Further large series and randomised controlled studies are needed on this subject.

DISCLOSURES

The authors report no conflict of interest.

AUTHOR CONTRIBUTIONS

Literature search: Murat Acat, Pinar Yildiz Gulhan, Serkan Oner, Muhammed Kamil Turan. Data collection: Murat Acat, Pinar Yildiz Gulhan, Serkan Oner, Muhammed Kamil Turan. Study design: Murat Acat, Pinar Yildiz Gulhan, Serkan Oner, Muhammed Kamil Turan. Analysis of data: Murat Acat, Pinar Yildiz Gulhan, Serkan Oner, Muhammed Kamil Turan. Manuscript preparation: Murat Acat, Pinar Yildiz Gulhan, Serkan Oner, Muhammed Kamil Turan. Review of manuscript: Murat Acat, Pinar Yildiz Gulhan, Serkan Oner, Muhammed Kamil Turan.

ORCID

Murat Acat  <https://orcid.org/0000-0002-7163-4882>

Pinar Yildiz Gulhan  <https://orcid.org/0000-0002-5347-2365>

Serkan Oner  <https://orcid.org/0000-0002-7802-880X>

Muhammed Kamil Turan  <https://orcid.org/0000-0002-1086-9514>

REFERENCES

1. Gulhan PY, Demirci N, Bozkus F, Yazici O, Coskun F. Interstitial lung diseases and COVID-19. *Eurasian J Pulmonol*. 2020;22:61-66.
2. Channappanavar R, Perlman S. Pathogenic human coronavirus infections: causes and consequences of cytokine storm and immunopathology. *Semin Immunopathol*. 2017;39:529-539.
3. Hosseiny M, Kooraki S, Gholamrezanezhad A, Reddy S, Myers L. Radiology perspective of coronavirus disease 2019 (COVID-19): lessons from severe acute respiratory syndrome and middle east respiratory syndrome. *AJR Am J Roentgenol*. 2020;214:1078-1082.
4. Udawadia ZF, Koul PA, Richeldi L. Post-COVID lung fibrosis: the tsunami that will follow the earthquake. *Lung India*. 2021;38:41-47.
5. Li YC, Bai WZ, Hashikawa T. The neuroinvasive potential of SARS-CoV2 may play a role in the respiratory failure of COVID-19 patients. *J Med Virol*. 2020;92:552-555.

6. Ferrara F, Granata G, Pelliccia C, La Porta R, Vitiello A. The added value of pirfenidone to fight inflammation and fibrotic state induced by SARS-CoV-2: anti-inflammatory and anti-fibrotic therapy could solve the lung complications of the infection? *Eur J Clin Pharmacol*. 2020;76:1615-1618.
7. Momen ABI, Khan F, Saber S, et al. Usefulness of pirfenidone in covid lung: a case series. *Eur J Med Health Sci*. 2021;3:24-26.
8. Ye Z, Zhang Y, Wang Y, Huang Z, Song B. Chest CT manifestations of new coronavirus disease 2019 (COVID-19): a pictorial review. *Eur Radiol*. 2020;30:4381-4389.
9. Pan F, Ye T, Sun P, et al. Time course of lung changes at chest CT during recovery from coronavirus disease 2019 (COVID-19). *Radiology*. 2020;295:715-721.
10. Sehirli E, Turan MK, Demiral E. A randomized automated thresholding method to identify comet objects on comet assay images. In: *Proceedings of the 3rd International Conference on Communication and Information Processing- ICCIP '17* [Internet]. ACM Press; 2017:464-467. [cited May 4, 2020].
11. Turan MK, Yücer E, Sehirli E, Karş İR. Estimation of population number via light activities on night-time satellite images. *Int Arch Photogramm Remote Sens Spatial Inf Sci*. 2017;XLII-4/W6:103-105.
12. Zayed N, Elnemr HA. Statistical analysis of haralick texture features to discriminate lung abnormalities. *Int J Biomed Imaging*. 2015;2015:1-7.
13. Mall PK, Singh PK, Yadav D. GLCM Based Feature Extraction and Medical X-RAY Image Classification using Machine Learning Techniques. In: *IEEE Conference on Information and Communication Technology*. 2019;2019:1-6. doi:10.1109/CICT48419.2019.9066263
14. Vasarmidi E, Tsitoura E, Spandidos DA, Tzanakis N, Antoniou KM. Pulmonary fibrosis in the aftermath of the COVID-19 era (Review). *Exp Ther Med*. 2020;20:2557-2560.
15. Zuo W, Zhao X, Chen YG. SARS Coronavirus and Lung Fibrosis. In: Lal S. (eds) *Molecular Biology of the SARS-Coronavirus*. Springer 2010, Berlin, Heidelberg. https://doi.org/10.1007/978-3-642-03683-5_15
16. Pittet JF, Griffiths MJ, Geiser T, et al. TGF-beta is a critical mediator of acute lung injury. *J Clin Invest*. 2001;107:1537-1544.
17. Ahmad Alhiyari M, Ata F, Islam Alghizzawi M, Bint I Bilal A, Salih Abdulhadi A, Yousaf Z. Post COVID-19 fibrosis, an emerging complication of SARS-CoV-2 infection. *IDCases*. 2021;23:e01041.
18. Seifirad S. Pirfenidone: a novel hypothetical treatment for COVID-19. *Med Hypotheses*. 2020;144:110005.
19. Mo X, Jian W, Su Z, et al. Abnormal pulmonary function in COVID-19 patients at time of hospital discharge. *Eur Respir J*. 2020;55:2001217.
20. Pogatchnik BP, Swenson KE, Sharifi H, Bedi H, Berry GJ, Guo HH. Radiology-pathology correlation in recovered COVID-19, demonstrating organizing pneumonia. *Am J Respir Crit Care Med*. 2020;202:598-599.
21. Tse GM, To KF, Chan PK, et al. Pulmonary pathological features in coronavirus associated severe acute respiratory syndrome (SARS). *J Clin Pathol*. 2004;57:260-265.
22. Zhang P, Li J, Liu H, et al. Long-term bone and lung consequences associated with hospital-acquired severe acute respiratory syndrome: a 15-year follow-up from a prospective cohort study. *Bone Res*. 2020;8:8.
23. Das KM, Lee EY, Singh R, et al. Follow-up chest radiographic findings in patients with MERS-CoV after recovery. *Indian J Radiol Imaging*. 2017;27:342-349.
24. Spagnolo P, Balestro E, Aliberti S, et al. Pulmonary fibrosis secondary to COVID-19: a call to arms? *Lancet Respir Med*. 2020;8:750-752.
25. Huang W, Wu Q, Chen Z, et al. The potential indicators for pulmonary fibrosis in survivors of severe COVID-19. *J Infect*. 2021;82:e5-e7.
26. Fang Y, Zhou J, Ding X, Ling G, Yu S. Pulmonary fibrosis in critical ill patients recovered from COVID-19 pneumonia: preliminary experience. *Am J Emerg Med*. 2020;38:2134-2138.
27. Guler SA, Ebner L, Aubry-Beigelman C, et al. Pulmonary function and radiological features 4 months after COVID-19: first results from the national prospective observational Swiss COVID-19 lung study. *Eur Respir J*. 2021;57:2003690.
28. Chaudhary S, Natt B, Bime C, Knox KS, Glassberg MK. Antifibrotics in COVID-19 lung disease: let us stay focused. *Front Med (Lausanne)*. 2020;7:539. doi:10.3389/fmed.2020.00539
29. Wigén J, Löfdahl A, Bjermer L, Elowsson-Rendin L, Westergren-Thorsson G. Converging pathways in pulmonary fibrosis and Covid-19 - the fibrotic link to disease severity. *Respir Med X*. 2020;2:100023.
30. Shihab Fuad S, Bennett William M, Hong YI, Andoh TF. Pirfenidone treatment decreases transforming growth factor-beta1 and matrix proteins and ameliorates fibrosis in chronic cyclosporine nephrotoxicity. *Am J Transplant*. 2002;2:111-119.
31. Grattendick KJ, Nakashima JM, Feng L, Giri SN, Margolin SB. Effects of three anti-TNF-alpha drugs: etanercept, infliximab and pirfenidone on release of TNF-alpha in medium and TNF-alpha associated with the cell in vitro. *Int Immunopharmacol*. 2008;8:679-687.
32. Li C, Han R, Kang L, et al. Pirfenidone controls the feedback loop of the AT1R/p38 MAPK/renin-angiotensin system axis by regulating liver X receptor-alpha in myocardial infarction-induced cardiac fibrosis. *Sci Rep*. 2017;7:40523.
33. Fois AG, Posadino AM, Giordo R, et al. Antioxidant activity mediates pirfenidone antifibrotic effects in human pulmonary vascular smooth muscle cells exposed to sera of idiopathic pulmonary fibrosis patients. *Oxid Med Cell Longev*. 2018;2018:2639081.
34. Giri SN, Leonard S, Shi X, Margolin SB, Vallyathan V. Effects of pirfenidone on the generation of reactive oxygen species in vitro. *J Environ Pathol Toxicol Oncol*. 1999;18:169-177.
35. Hamidi SH, Kadamboor Veethil S, Hamidi SH. Role of pirfenidone in TGF-beta pathways and other inflammatory pathways in acute respiratory syndrome coronavirus 2 (SARS-Cov-2) infection: a theoretical perspective. *Pharmacol Rep*. 2021;73:712-727.
36. Umemura Y, Mitsuyama Y, Minami K, et al. Efficacy and safety of nintedanib for pulmonary fibrosis in severe pneumonia induced by COVID-19: an interventional study. *Int J Infect Dis*. 2021;108:454-460.

How to cite this article: Acat M, Yildiz Gulhan P, Oner S, Turan MK. The performance of artificial intelligence supported Thoracic CT to evaluate the radiologic improvement in patients with COVID-19 pneumonia: Comparison pirfenidone vs corticosteroid. *Int J Clin Pract*. 2021;75:e14961. doi:[10.1111/ijcp.14961](https://doi.org/10.1111/ijcp.14961)